MODELLING THE HEATING AND COOLING CYCLES OF A SODIUM SULPHUR BATTERY

***A. Safar[1], M. Vasey[1], P. J. Heggs[1].**

[1]Department of Chemical Engineering, University of Leeds, Leeds, LS2 9JT, UK

Abstract The heating and cooling processes of sodium-sulphur (NaS) batteries in a laboratory furnace are investigated from room temperature to 340°C. The heating and cooling of the battery is modelled in MATLAB by discretizing the Fourier equation using the fully implicit backward finite difference method. The Stefan problem with regards to the phase change is approximated with the apparent heat capacity method [1]. The aim of the modelling is to shorten start up time and increase efficiency.

Keywords: NaS battery, Fourier equation, Stefan problem, Apparent heat capacity, Thermal radiation, Numerical solution

1. INTRODUCTION

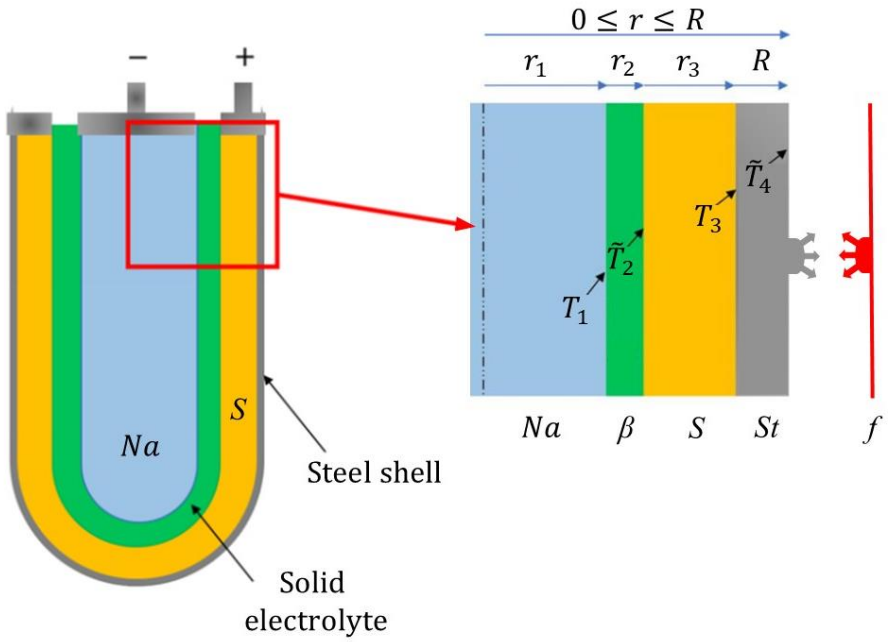

Figure 1: Battery diagram.

The sodium-sulphur battery comprises four layers: an inner core of sodium (Na), a beta alumina dividing membrane (β), an annulus of sulphur (S) and an outer steel casing (St). The battery is heated in an insulated furnace at a constant rate and allowed to cool naturally. The furnace is heated from room temperature up to 300-350°C, at which the electrical charging and discharging of the battery occur. The sodium melts at 97.8°C, and the sulphur at 115°C. The sulphur electrode has the biggest influence on heat transfer, as it has the highest thermal resistance. To avoid problems, the sodium and the sulphur melting phases are desired to not overlap. Convection in the furnace is ignored, as the battery is heated and cooled by thermal radiation effects. Experimental data of furnace and battery temperatures have

*Corresponding Author: pm20a2s@leeds.ac.uk

been collected over the complete cycle and the predictions of the temperatures of the battery layers by a numerical simulation are presented.

2. EXPERIMENTAL PROCEDURE

Table 1: Battery specifications.

Parameters	Values
Sodium layer radius (r_1)	7.7 mm
Radius up to the beta alumina layer (r_2)	9.7 mm
Radius up to the sulphur layer (r_3)	13.3 mm
Battery radius ($r_4 = R$)	16 mm

The furnace battery apparatus that is desired to model is used to fit the cooling data. This is done in order to simplify the model, as the experimental data will encapsulate all the factors associated with natural cooling. The battery is heated based on the recommended specifications where the battery is initially heated from room temperature to 100℃ at 1℃ per minute. Then the furnace temperature is held constant for 1 hour to allow for the sodium to melt prior to heating again at 1℃ per minute to 160℃. After reaching 160℃ the furnace temperature is held constant again to allow for the sulphur layer to melt. Finally, the furnace temperature is increased to 340℃ at 1℃ per minute to reach an operational battery temperature. The furnace temperature is kept constant for an hour in order to equilibrate the temperature of the battery prior to natural cooling. During the experiment, a thermocouple and a data logger are used to measure and log the furnace temperature. The data for the battery furnace temperature during cooling is regressed, and incorporated in the model based on the fitted experimental equation equ. (11) to represent the cooling temperature profile.

3. MATHEMATICAL MODEL

The mathematical model is constructed with the assumptions that conduction occurs with radial symmetry in an infinitely long cylinder and the four layers are in intimate contact and thermal radiation occurs to and from the steel casing and the furnace. The 2D Fourier equation in (*t*,*r*) for a very long cylinder equ. (1) is applied for each layer comprising the battery with i = 1, 2, 3 and 4 for the sodium, beta alumina, sulphur and steel casting respectively.

$$\left(\rho c_p\right)_i \frac{\partial T_i}{\partial t} = \lambda_i \left\{\frac{1}{r}\frac{\partial T_i}{\partial r} + \frac{\partial^2 T_i}{\partial r^2}\right\} \tag{1}$$

with an initial condition:

$$\text{at } t \le 0, T_i = T_f = T_{in} \text{ over } 0 \le r_1 \le r_2 \le r_3 \le r_4 = R \tag{2}$$

The boundary conditions are:

$$\text{for } t > 0, \text{at } r = 0, \frac{\partial T_i}{\partial r} = 0 \text{ and at } r_i, -\lambda_i \frac{\partial T_i}{\partial r} = \lambda_{i+1} \frac{\partial T_{i+1}}{\partial r} \; and \; T_i = T_{i+1} \text{ , for } i = 1, 2 \text{ and } 3 \tag{3}$$

$$\text{and at } r = r_4 = R, \qquad -\lambda_4 \frac{\partial T_4}{\partial r} = \mathcal{F}_{4\to f}\sigma\left(T_4^4 - T_f^4\right) \tag{4}$$

$$\text{and finally,} \qquad T_f = \text{fn}\,(t) \tag{5}$$

For the phase changes that occur in layers 1 and 2 (sodium and sulphur), equ. (1) is used to represent the Stefan problem. The heat capacity is increased to account for the latent heat over a small temperature interval by equ. (6) [1]as follows:

$$c_{app} = \left(\int_{T_{1\mathrm{sf}}}^{T_{2\mathrm{sf}}} c_{\mathrm{p}} \, \mathrm{d}T + h_{\mathrm{sf}} \right) / (T_{2\mathrm{sf}} - T_{1\mathrm{sf}}) \tag{6}$$

where c_{app} is the apparent heat capacity, h_{sf} is the latent heat of fusion and the phase change occurs over the small temperature interval $(T_{2\mathrm{sf}} - T_{1\mathrm{sf}})$.

The thicknesses of the beta alumina and the steel casting are much smaller than the other layers and with relatively large values of thermal conductivity are represented by average temperature values - $\tilde{T}_2$ and $\tilde{T}_4$ respectively. The average temperatures are defined as follows with i = 2 and 4:

$$\tilde{T}_i = 2 \left(\int_{r_{i-1}}^{r_i} T_i(r) r \, dr \right) / \left(r_i^2 - r_{i-1}^2 \right) \tag{7}$$

Combining equ. (7) with equ. (1) and equs (4) for i = 2 results in an ordinary differential equation for the average temperature of the beta alumina layer as follows:

$$\left(\rho c_p\right)_2 \times \frac{1}{2} \left(r_2^2 - r_1^2 \right) \frac{\mathrm{d}\tilde{T}_2}{\mathrm{d}t} = \lambda_3 r_2 \frac{\partial T_3}{\partial r} - \lambda_1 r_1 \frac{\partial T_1}{\partial r} \tag{8}$$

and for the steel casting, combining equ. (7) with equ. (1), equs (4) and (5) for i = 4 provides the following equation for the average temperature of the steel casting:

$$\left(\rho c_p\right)_4 \times \frac{1}{2} \left(r_4^2 - r_3^2 \right) \frac{\mathrm{d}\tilde{T}_4}{\mathrm{d}t} = r_4 \alpha_{rad} (T_4 - T_{\mathrm{f}}) - \lambda_3 r_3 \frac{\partial T_3}{\partial r} \tag{9}$$

where the radiative heat transfer coefficient α_{rad} has been introduced into equ. (5) and is defined as

$$\alpha_{rad} = \mathcal{F}_{4 \to f} \sigma \left(T_4^4 - T_f^4 \right) / (T_4 - T_{\mathrm{f}}) \tag{10}$$

The cooling temperature profile is represented by the following fitted equation:

$$T_f = 5.284 \times 10^{-17} \times t^4 - 8.774 \times 10^{-12} \times t^3 + 5.982 \times 10^{-7} \times t^2 - 0.02077 \times t + 340 \tag{11}$$

where the adjusted R square is 0.9995 and t is the time starting when the furnace heating has been turned off.

The complete set of partial and ordinary differential equations are overall non-linear due to the radiative transfer of heat. The equations (1) to (5), (8) and (9) are solved numerically using the fully implicit back methodology [2] and the ordinary different equations by back difference approximation. Iteration at every time increment is required until the radiation heat transfer coefficient α_{rad} agrees to a tolerance of 0.001 W m^{-2} K^{-1}. The set of algebraic equations were determined to be stable based on von Neumann's method [2]. The numerical solution was developed using MATLAB software and run on a desk top computer with 16 GB ram and computing times for simulations of 18 hours of experimental data took 6.5 hours.

4. RESULTS

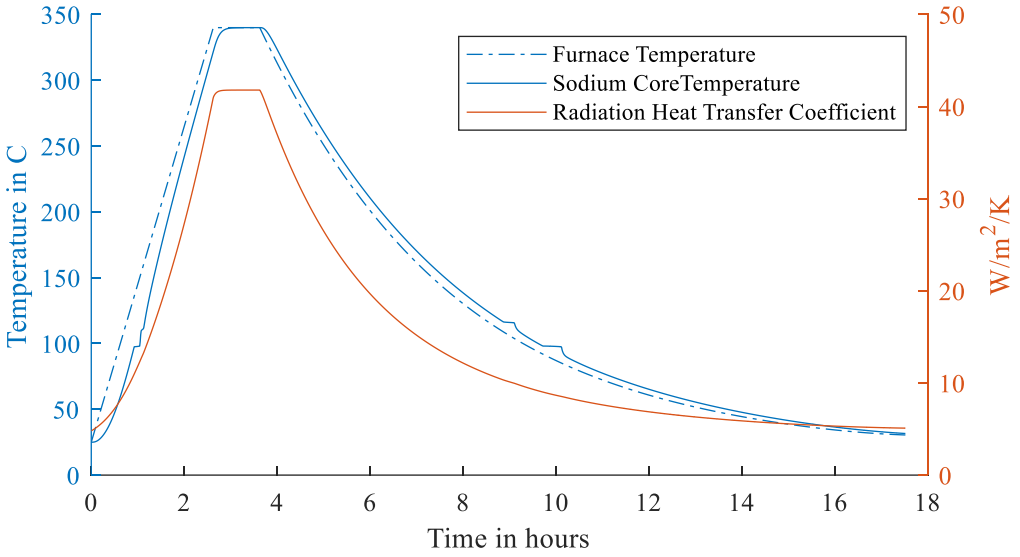

Figure 2: The modelled heating (2℃/min) and cooling of the sodium sulphur battery.

The mathematical model has been used to simulate a multitude of heating scenarios from 25℃ up to 340℃. Previously, the recommended safe operating regime was heating at 1℃ per minute up to 100℃, hold for 1 hour, then heat again at 1℃ per minute up to 160℃ and hold for 1 hour, and then, finally heat again at 1℃ per minute until 340℃ is reached. At this point, the system was allowed to come to thermal equilibrium before cooling occurred naturally. Unfortunately, the duration of the heating part of the cycle was too long for safe University laboratory practice – heating combustible materials outside normal hours and thus the simulation has been used to predict the possible safe heating regimes in much shorter time. The heating was simulated with and without holding the furnace temperature constant over the melting temperature regimes until each layer is fully melted. Holding the furnace temperature was found to be unnecessary at heating the battery. Heating rates of 2℃/min and 3℃/min were found to be effective at heating the battery relatively quickly and efficiently without any overlap between the phase changing regimes of the sodium and sulphur.

Results obtained from heating at 2℃/min are presented in figures 2 and 3 respectively. In figure 2, the rate of heating of the sodium layer increases gradually in the beginning, as the intermediate layers are starting to heat up from room temperature. After steadily heating the layers the heating rate of the sodium layer becomes constant until the phase changing regime is reached. The sodium core temperature remains constant during the phase change, which matches expectations of what would happen. After reaching a furnace temperature of 340℃ the furnace temperature is kept constant for an hour to replicate the experimental procedure to equilibrate the temperatures before the natural cooling of the furnace occurs. The cooling temperature profile in the simulation is based on the fitted experimental data from equation (11). During cooling two distinct flat regions are observed in the sodium core temperature, which coincide with the phase changing regimes. The radiation heat transfer coefficient is highly correlated with the rising and falling of the furnace temperature, which is due to the high dependence on temperature in equation (10).

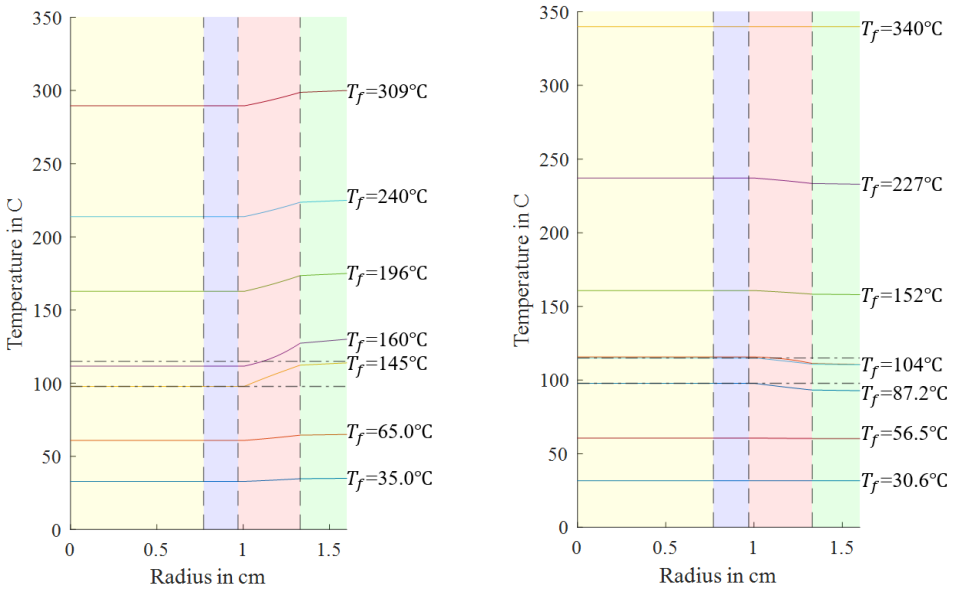

Figure 3: A multitude of battery temperature profiles during heating (a) (2℃/min) and cooling (b) where the yellow shading is the sodium layer, the blue shading is the beta alumina layer, the red shading is the sulphur layer, the green shading is the steel layer, T_f is the furnace temperature and the horizontal dash-dot lines represent the phase change temperatures.

In figure 3, the temperature profile across the sulphur layer is the largest, because it has the lowest value of thermal conductivity and thus, the largest thermal resistance in the battery. Moreover, the temperature gradient widens at the phase changing regimes, due to the latent heating. The heating process has larger gradients compared to the cooling process, as the battery is externally heated at a higher rate compared to the natural cooling rate. The total heating times at 2℃/min and 3℃/min are 2.63 and 1.75 hours respectively, which are considerably less than the earlier procedure of approximately 7 hours.

5. CONCLUSIONS

In conclusion, a model that simulates the heating and cooling of NaS batteries is developed, by discretizing Fourier's law of conductivity using the fully implicit backward Euler method. The model can be used to examine the temperature profile of the battery at different heating stages and recommend heating procedures. It was shown that heating NaS batteries at 2℃/min and 3℃/min would provide fast and efficient start up without overlapping the phase changing regimes. The results represent a significant improvement to the current heating process and enables more time to investigate the charging and discharging of the battery at the high temperature during a full day in the laboratory

NOMENCLATURE

Symbol	Definition
Roman	
c_p	Specific heat capacity (J kg^{-1} K^{-1})
c_{app}	Apparent heat capacity (J kg^{-1} K^{-1})
$\mathcal{F}$	View factor
f	Furnace
h_{sf}	Latent heat of fusion (J kg^{-1})
Na	Sodium
NaS	Sodium-sulphur
R	Battery radius (m)
r	Radius (m)
S	Sulphur
St	Steel
T	Temperature (K or ℃)
t	Time (s)
Greek	
α	Radiative heat transfer coefficient (W m^{-2} K^{-1})
β	Beta-alumina
λ	Thermal conductivity (W m^{-1} K^{-1})
ρ	Density (kg m^{-3})
σ	Stefan-Boltzmann constant (W m^{-2} K^{-4})
Superscripts	
$\sim$	Average
Subscripts	
i	Layer index

ACKNOWLEDGEMENTS

I gratefully acknowledge the financial support from the Kuwait Ministry of Higher Education, which facilitated the study of the Advanced Chemical Engineering MSc program at the University of Leeds.

REFERENCES

[1] POIRIER, D. and SALCUDEAN, M. 1988. On numerical methods used in mathematical modelling of phase change in liquid metals. *Journal of Heat Transfer*, 110, 562-570

[2] SMITH, G. D. 1985. *Numerical solution of partial differential equations: finite difference methods*, Oxford University Press.